2016-09-01

Hybrid Wave and Offshore Wind Farms: a Comparative Case Study of Co-located Layouts

Astariz, S

International Journal of Marine Energy

Hybrid Wave and Offshore Wind Farms: a Comparative Case Study of Co-located Layouts

S. Astariz[#1], C. Perez-Collazo[*2], J. Abanades[*3], G. Iglesias[*4]

[#]*EPS, Hydraulic Engineering, University of Santiago de Compostela, Spain*

[1]sharay.astariz@usc.es

[*]*School of Marine Science and Engineering, Plymouth University, Plymouth, UK*

[2]carlos.perezcollazo@plymouth.ac.uk

[3]javier.abanadestercero@plymouth.ac.uk

[4]gregorio.iglesias@plymouth.ac.uk

Abstract

Marine energy is one of the most promising alternatives to fossil fuels due to the enormous energy resource available. However, it is often considered uneconomical and difficult. Co-located offshore wind turbines and wave energy converters have emerged as a solution to increase the competitiveness of marine energy. Among the benefits of co-located farms, this work focuses on the shadow effect, i.e. the reduction in wave height in the inner part of the farm, which can lead to significant savings in operation and maintenance (O&M) costs thanks to the augmented weather windows for accessing the wind turbines. The aim of this study is to quantify the wave height reduction achieved within a co-located wave-wind farm. Different locations and a large number of layouts are analysed in order to define the optimum disposition.

Keywords: Wave energy; Wind energy; Co-located wind–wave farm; Weather windows for O&M; Shadow effect; Wave height.

1. Introduction

If wave energy is to become a viable alternative to fossil fuels, its competitiveness must be enhanced. Combining this promising marine renewable with a more consolidated renewable like offshore wind energy is a solution of great interest [1]. According to the degree of connectivity between the offshore wind turbines and Wave Energy Converters (WECs) combined wave-wind systems can be classified into: co-located, hybrid and islands systems [2]. According to the current state of development of both technologies, the co-location of WECs into a conventional offshore wind farm is regarded as the best option [2], which combines an offshore wind farm and a WEC array with independent foundation systems but sharing: the same marine area, grid connection, O&M equipment, etc.

There are many synergies between both renewables [3], such as the more sustainable use of the marine resource, the reduction in the intermittency inherent to renewables or the opportunity to reduce costs by sharing some of the most expensive elements of an offshore project. In addition to these powerful reasons there are a number of technology synergies between wave and wind systems which make their combination even more attractive, and this paper focuses on one of them: the so-called shadow effect, i.e. the reduction of the significant wave height in the inner part of the farm. The operational limit of workboats (the most cost-effective access system for maintenance tasks) is a significant wave height of 1.5 m [4]; when this threshold is exceeded delays in maintenance and repairs ensue, increasing downtime – with the associated costs. Thus, while modern onshore wind turbines present accessibility levels of 97% [5], this level can be significantly reduced in offshore installations .

On this basis, the aim of this study is to analyse the wave height reduction achieved by deploying co-located WECs and the influence of the layout in the results. This purpose is carried out through various cases studies. First, a number of hypothetical co-located farms are analysed in the Wave Hub area. Second, a real wind farm, Alpha Ventus, is considered in order to obtain more realistic conclusions. Finally, the

study extends to three other wind farms currently in operation (Bard 1, Horns Rev 1 and Lincs) to compare the results obtained for each site and draw general conclusions about the benefit of co-located farms and the optimum layouts. A state-of-the-art, third generation wave propagation model (SWAN) implemented on a high-resolution computational grid is applied and real sea conditions are considered.

2. Methodology

2.1. Preliminary Case Study

This case study was carried out for a hypothetical wind farm at the Wave Hub site, an offshore renewable energy (ORE) test centre 20 km to the northwest of St Ives Bay, in SW England (Figure 1).

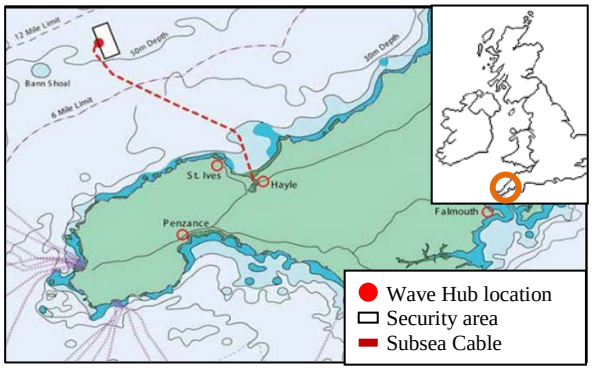

Figure 1. Wave Hub location [6].

The water depth at the test site ranges between 40 and 60 m [7]. As regards the sea climate, three wave conditions were defined (Table 1) on the basis of the most recent available data [8].

Table 1. Case Study (CS): H_s = significant wave height; T_p = peak period; θ = mean wave direction.

CS	H_s (m)	T_p (s)	θ (º)
1	1.5	7.57	270
2	2.5	8.14	270
3	3.5	9.33	270

The wind farm layout is based on that of Horns Rev 1, with 80 turbines (Vestas V80-2MW) erected on a grid with 10 rows. The spacing between adjacent turbines and rows is 560 m [9]. Thus, the proposed wind farm would occupy a total area of approximately 20 km^2 with an average water depth of 50 m. The substructure of the wind turbines is jacket-frames of 18 m x 18 m. The wind farm is staggered and orientated taking into account the main wind direction in the area in order to maximise the energy output.

Having defined the wind farm layout, a Peripherally Distributed Array (PDA) was selected for the co-location of the WECs. The PDA is a type of co-located system which combines both wind and wave arrays by positioning the WECs at the periphery of the offshore wind farm.

The WEC used in this case study, and in the following cases, is WaveCat: a floating offshore WEC whose principle of operation is wave overtopping, and with a length overall of 90 m. The minimum distance between devices is 2.2D, where D = 90 m is the distance between the twin bows of a single WaveCat WEC [10, 11].

14 wave farm configurations were proposed: 3 basic layouts (named A, B, C) with different spacing between devices: configuration A, with a spacing between WECs equal to that between turbines, 560 m; configuration B, with a smaller spacing, 345 m; and configuration C, with the minimum spacing allowed, 198 m. For each of these basic configurations, different layouts were considered (Figure 2): (i) two rows of devices along the west side of the wind farm; (ii) two rows along the west side plus two additional rows of devices along the north and south sides, at an angle of 45°; (iii) two rows of devices forming an arch; and (iv) two rows of devices along an arch rotated 11° clockwise. These configurations were used to investigate the influence of the layout on the wave characteristics within the wind farm, and more specifically the influence of the spacing between devices and the addition of new lateral rows of devices to intercept waves from secondary directions (NW and SW), and to ascertain whether an arch layout can achieve a similar wave height reduction to an angular layout with fewer WECs.

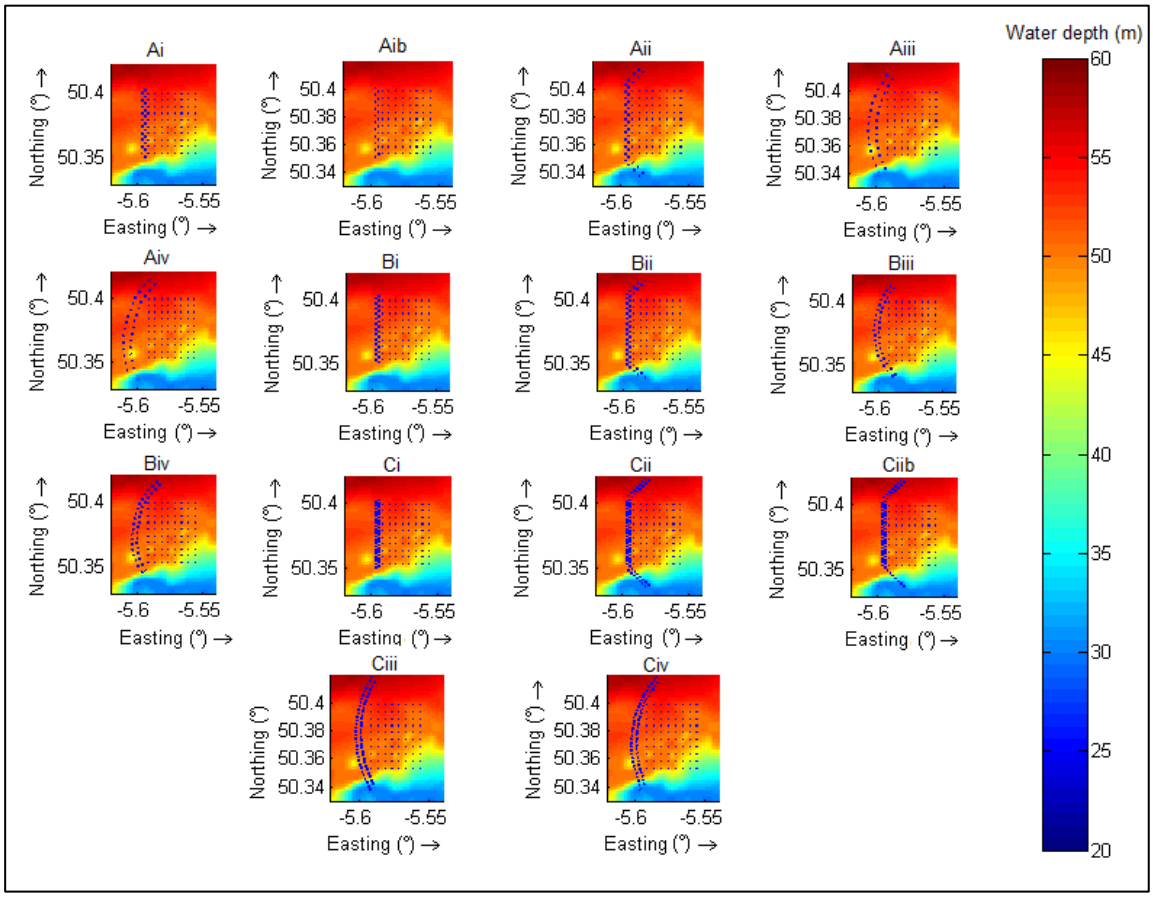

Figure 2. Co-located farms at the Wave Hub site: configurations A_i to C_{iv}.

2.2. Realistic Case Study

Next, the shadow effect provided by co-located WECs added to an existing wind farm, Alpha Ventus, was investigated using one year's worth of buoy data (from January 2013 to December 2013) from the FINO1 research platform, only 400 m away from the farm (Figure 3) [12]. This park lies about 45 km north of the island of Borkum (Germany), in water depths of approx. 30 m [13]. The Alpha Ventus wind farm is composed by 12 turbines: 6 AREVA turbines with a tripod substructure and 6 Repower 5M turbines with a jacket-frame substructure with a spacing between turbines of around 800 m [14]. In this case, 15 wind-wave farms configurations were tested (Table 2, Figure 4) characterised by different spacing between WECs, disposition and number of devices (N_{WECs}).

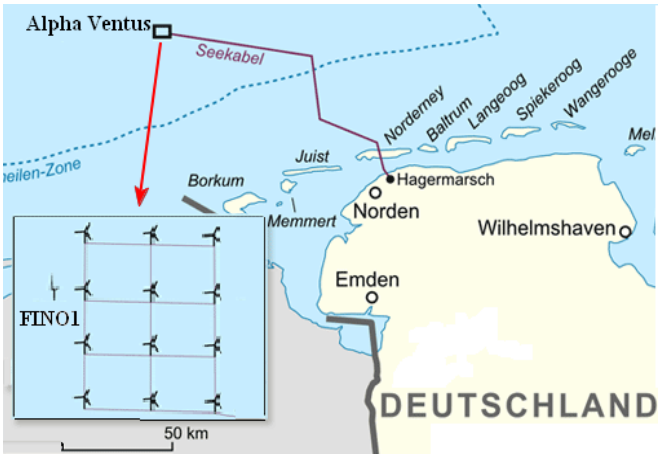

Figure 3. Alpha Ventus location [12].

Table 2. Characteristics of the WEC layouts

Spacing	Name	N_{WEC}	Short description
750 m	A_i	9	Two rows to the NW.
	A_{ii}	12	Two rows to the NW and two more rows to the W.
	A_{iii}	12	Arch to the NW.
450 m	B_i	12	Two rows to the NW.
	B_{ii}	17	Two rows to the NW and two more rows to the W.
	B_{iii}	17	Arch to the NW.
198 m	C_i	22	Two rows to the NW
	C_{ii}	30	Two rows to the NW and two more rows to the W.
	C_{iii}	28	Arch to the NW.
198 m	C_{ib}	27	Two rows to the NW and one more row to the SW of the farm constituted by 5 additional WECs.
	C_{ic}	31	Two rows to the NW and two more rows to the SW of the farm constituted by 9 additional WECs.
	C_{iib}	32	Two rows to the NW and two to the W (2 additional WECs).
	C_{iic}	34	Two rows to the NW and two to the W (4 additional WECs).
	C_{iiib}	30	Arch to the NW (2 additional WECs).
	C_{iiic}	32	Arch to the NW with 4 additional WECs.

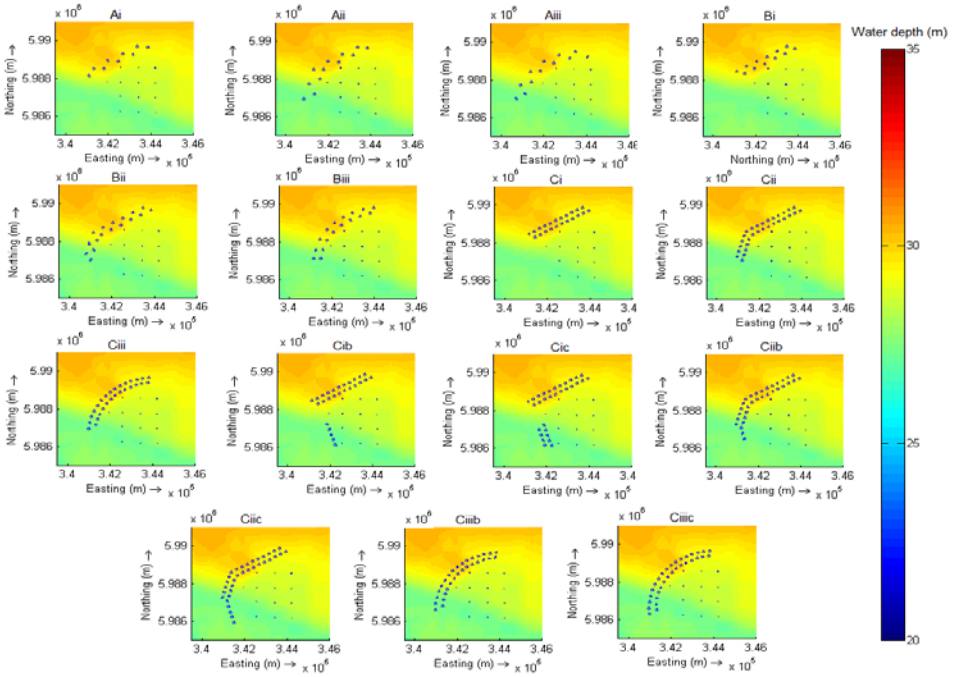

Figure 4. Co-located wave-wind farm layouts in Alpha Ventus (configurations A_i to C_{iiic}) and water depth (m).

2.3. Comparative Study

The results of the previous study of AlphaVentus were taken as a reference for three further cases, corresponding to as many wind farms currently in operation: Bard 1, Horns Rev 1 and Lincs, whose locations and characteristics are presented in Figure 5 and Table 3, respectively. These four wind farms encompass a wide variety of characteristics on which to establish a comparative analysis.

Figure 5. Location of the four wind farms used in this study: Alpha Ventus, Bard 1, Horns Rev 1 and Lincs.

Table 3. Characteristics of the wind farms

Wind farm	Depth (m)	Distance from shore (km)	Installed capacity (MW)	Number turbines	Area (km^2)
Alpha Ventus	33-45	56	60	12	4
Bard 1	39-41	90-101	400	80	59
Horns Rev 1	6-14	14-20	160	80	21
Lincs	8-16	8	270	75	41

Alpha Ventus and Horns Rev have been characterised previously. For their part, Bard 1 is composed of 80 5 MW turbines (Bard 5.0) on tripod substructures [15], and Lincs of 75 3.6 MW Siemens turbines on monopiles [16]. In Alpha Ventus and Horns Rev 1 the wind turbines are arranged on a Cartesian grid, whereas in Bard 1 and Lincs they are not organised in clearly defined rows, and the distance between turbines varies in each case. As regards the sea climate, wave buoy measurements were used, and the main wave climate parameters are shown in Table 4: H_s is the significant wave height, T_{m01} the mean wave period, θ the mean wave direction, U_w the most frequent wind speed at 10 m, and D_w the corresponding wind direction.

Table 4.Wave and wind conditions at the wind farm site.

Wind farm	H_s (m)	T_{mo1} (s)	θ (º)	U_w(ms^{-1})	D_w (º)
Alpha Ventus	1.5	4.6	330	10	210-240
Bard 1	0.8-1.5	4.0	320	9.2	330
Horns Rev 1	0.8-1	4-4.6	230-340	9.7	225-315
Lincs	0.6-0.7	3.4-4.4	0-15	8.4	10-70

Two co-located WECs layouts (Table 5) were proposed taking into account the wind farm layouts, the wave climate, and the results of previous studies. In the first case (Figure 6), the co-located WECs configuration consists of two main rows of WECs with a spacing of 198 m orientated towards the prevailing wave direction, and other rows of WECs at an angle of 45º to face secondary wave directions and thus protect a larger wind farm area. With the second configuration (Figure 7) the aim is to check if

deploying WECs in an arch can lead to a wave height reduction similar to that obtained with an angular layout with fewer WECs.

Table 5. Total number of co-located WECs and the rate between the total number of WECs and wind turbines (*r*).

Wind farm	Layout in angle		Layout in arch	
	Total	*r*	Total	*r*
Alpha Ventus	34	2.83	32	2.67
Bard 1	79	0.99	79	0.99
Horns Rev 1	55	0.69	53	0.66
Lincs	81	1.01	80	1

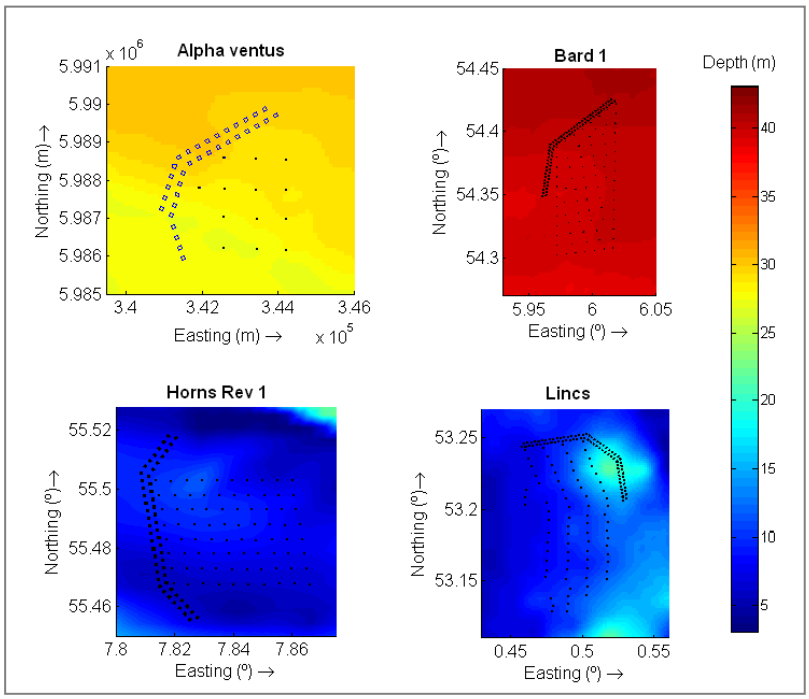

Figure 6. Co-located wind farm layouts with WECs at an angle.

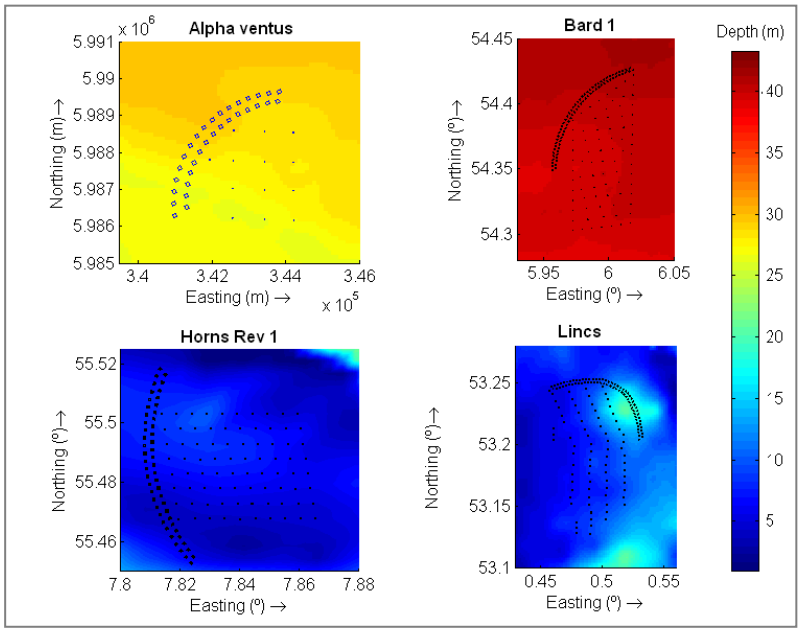

Figure 7. Co-located wind farms layouts with WECs in arch.

2.4. The Wave Propagation Model

The assessment of the wave height reduction in the wind farm caused by the co-located WECs was carried out using a third-generation numerical wave model, SWAN (Simulating WAves Nearshore), which was successfully used in previous works (e.g. [17-19]) to model the impact of a wave farm on nearshore wave conditions. The evolution of the wave field is described by the action balance equation, Eq. (1), which equates the propagation of wave action density in each dimension balanced by local changes to the wave spectrum:

$$\frac{\partial}{\partial t} N + \frac{\partial}{\partial x} c_x N + \frac{\partial}{\partial y} c_y N + \frac{\partial}{\partial \sigma} c_\sigma N \frac{\partial}{\partial \theta} c_\theta N = \frac{S_{tot}}{\sigma} \quad (1)$$

where t is time (s), c_x and c_y are spatial velocities in the x and y components (ms^{-1}), c_θ and c_σ are rates of change of group velocity which describe the directional (θ) rate of turning and frequency (σ) shifting due to changes in currents and water depth, N is wave action density spectrum, and S_{tot} is the energy density source terms which describe local changes to the wave spectrum.

In this work the model was implemented in the so-called nested mode, with two computational grids (Table 6) in order to obtain high-resolution results without excessive computational cost. The bathymetric data, from the UK's data centre Digimap, were interpolated onto this grid.

Table 6. Surface area covered by the computational grids and grid size.

Wind farm	Coarse grid		Nested grid	
	Area (km)	Resolution (m)	Area (km)	Resolution (m)
Alpha Ventus	40 × 30	100 × 100	8.5 × 8.5	17 × 17
Bard 1	111 × 111	222 × 222	18 × 22	40 × 40.4
Horns Rev1	42 × 32	70 × 80	9.35 × 9	17 × 20
Lincs	119 × 111	170 × 159	14.4 × 18.2	32 × 33

The wind turbines were represented in the model by a transmission coefficient, whose value can vary in theory from 0% (i.e., 100% of incident wave energy absorbed) to 100%. This technique was used in previous studies to represent single wind turbines [20] or wind farm arrays [21], and arrays of WECs [22]. In this study, the transmission coefficient of the offshore wind turbines was calculated by [23]:

$$c_t = 4\left(\frac{d}{H_i}\right) E\left[-E + \sqrt{E^2 + \frac{H_i}{2d}}\right] \quad (2)$$

$$E = \frac{C_d\left(\frac{b}{D+b}\right)}{\sqrt{1-\left(\frac{b}{D+b}\right)^2}} \quad (3)$$

where d is depth (m), H_i is incident significant wave height (m), D is the pile diameter (m), b is the pile spacing (m), and C_d is the drag coefficient of the piles (1.0 for a smooth pile).

As for the co-located WECs, the WEC used was the WaveCat, and its wave transmission coefficient was implemented into the wave propagation model based on the laboratory tests reported by Fernandez, Iglesias [11].

2.5. Impact Indicators

To compare the results achieved in the proposed co-located farms a series of impact indicators were defined: (i) the significant wave Height Reduction within the Farm (*HRF*), (ii) the significant wave Height

Reduction within the *j*-th Area of wind turbines (*HRAj*), and (iii) the increase in access time for O&M ($\Delta T_{O\&M}$). The *HRF* and HRA_j indices provide information about the average wave height reduction within the wind farm and the wave recovery with increasing distance from the WECs, respectively, and were calculated by

$$HRF\ (\%) = \frac{100}{n}\sum_{i=1}^{n}\frac{1}{(H_{s,b})_i}\left[(H_{s,b})_i - (H_{s,W})_i\right] \quad (4)$$

where the index *i* designates a generic turbine of the wind farm, *n* is the total number of turbines, $(H_{s,b})_i$ is the significant height incident on the *i*-th turbine in the baseline scenario (without WECs), and $(H_{s,W})_i$ is the significant height incident on the *i*-th turbine with co-located WECs.

$$HRA_j(\%) = \frac{100}{m}\sum_{i=1}^{m}\frac{1}{(H_{s,b})_i}\left[(H_{s,b})_i - (H_{s,W})_i\right] \quad (5)$$

where the index *i* denotes a generic turbine of the *j*-th area of the wind farm, and *m* is the number of turbines in the *j*-th area. In the case of Alpha Ventus and Horns Rev 1 each *j*-th area corresponds to a vertical row of turbines numbered from east to west, *j* = 1, 2, 3 in Alpha Ventus and *j* = 1, 2…10 in Horns Rev 1. However, in the other two wind farms, due to the less orderly layout, the division was made into different areas with a similar number of turbines, and numbered according to the mean wave direction (Figure 8).

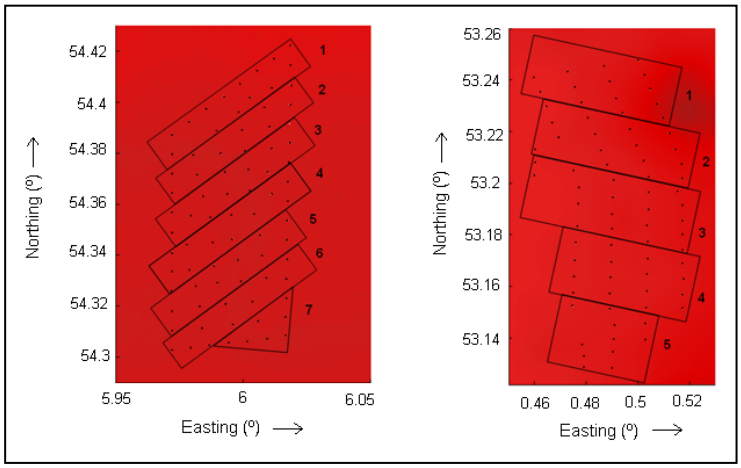

Figure 8. The *j*-th areas into which Bard 1 (left) and Lincs (right) were divided to calculate the HRA_j index.

The $\Delta T_{O\&M}$ non-dimensional index allows the assessment of the increase in the timeframe accessibility to the wind turbines thanks to the co-located WECs, and can be computed from

$$\Delta T_{O\&M}(\%) = \frac{T_W - T_b}{T_W} \times 100 \quad (6)$$

where T_W and T_b are the total number of hours per year when H_s within the wind farm is lower or equal to 1.5 m with co-located WECs and in the baseline scenario, respectively.

3. Results and Discussion

3.1. Preliminary Study

As regards the wave height reduction (Table 7), a value of *HRF* between 12% (A_{ib}) and 24% (C_i) was obtained for the configurations X_i, with X=A, B, C. In the case of 560 m as spacing between devices, two situations were analysed (A_i and A_{ib}) in order to evaluate the difference between aligning the devices of the first or second row with the wind turbines. *HRF* values were higher in the first case (A_i), and therefore this arrangement was retained for all the other layouts.

Table 7. *HRF* (%) values for case studies CS1, CS2 and CS3 and configurations A_i to C_{iv}.

Configuration	CS1	CS2	CS3
A_i	13	13	13
A_{ib}	12	12	12
B_i	16	16	16
C_i	24	24	24
A_{ii}	14	14	14
B_{ii}	18	18	18
C_{ii}	26	26	26
C_{iib}	25	25	25
A_{iii}	11	11	11
B_{iii}	17	17	17
C_{iii}	25	25	25
A_{iv}	15	15	15
B_{iv}	17	17	17
C_{iv}	27	27	28

The configurations with two more rows of 7 WECs at an angle of 45º (X_{ii}, with X=A, B, C) led to higher *HRF* values than the corresponding Xi configurations, increasing the wave reduction by 6-8%. Indeed, a barrier of WECs to the northwest and southwest of the farm is essential to intercepting the waves from these directions, and to retard wave regeneration within the farm. As regards the layout with the smallest spacing, 198 m (C_{ii}), the average *HRF* value was 26% for C_{ii} and 25% C_{iib}, indicating that that the second row to the south does not contribute to the wave height reduction, and therefore is not worth being included.

In the X_{iii} configurations, with an arched WEC layout, *HRF* values were a little lower than in the X_{ii} configurations. The explanation may lie in the reduction of the number of converters and in the fact that NW waves are not well intercepted. However, when the arch was rotated (X_{iv} configurations) the highest value of *HRF* was obtained – the C_{iv} configuration, with an average value of *HRF* of 27%. This could be caused by the refraction of the waves in the vicinity of the wind farm, veering from west to northwest.

In brief, the greatest wave height reduction was obtained for the minimum spacing between devices – *HRF* values are around50% greater than those achieved in the configurations with the maximum spacing.

Moreover, deploying WECs not only along the W side of the farm but also along its SW and NW sides reduces the wave height by more than 13%. Finally, arched configurations require fewer WECs for equivalent levels of wave height reduction.

3.2. Realistic Case Study

First, the results obtained from the nearshore wave propagation model were successfully validated with the wave data from the FINO1 platform, as demonstrated by the values obtained for the coefficient of determination (R^2) and the Root Main Square Error (*RMSE*): R^2 = 0.95 and *RMSE* = 0.36 m.

Having validated the numerical model, it was used to analyse the shadow effect caused by the 9 basic wind-wave farm layouts (A_i to C_{iii}). First, the prevailing sea climate was considered in these simulations – Case Study 1 (CS1): H_s = 1.5 m, T_p = 6.5 m and θ = 330° – to draw initial conclusions about the configuration that would maximise the weather windows for O&M. Second, and to cover the secondary wave direction, the same simulations were carried out but considering southwestly waves – CS2: H_s = 1.5 m, T_p = 6.5 m and θ = 250°.

The results are shown graphically in Figure 9 and 10, and numerically in Table 8. Comparing the different layouts, there was a small difference between configurations X_{ii} and X_{iii}, whereas poorer results were obtained for the configurations X_i. Regarding the influence of the spacing between devices, the configurations C_x led to the largest reductions. Based on these assessments and with the objective of a better protection from W and SW waves, 6 new configurations ($C_{ib,c}$, $C_{iib,c}$ and $C_{iiib,c}$) were analysed, consisting in variants of C_x layouts.

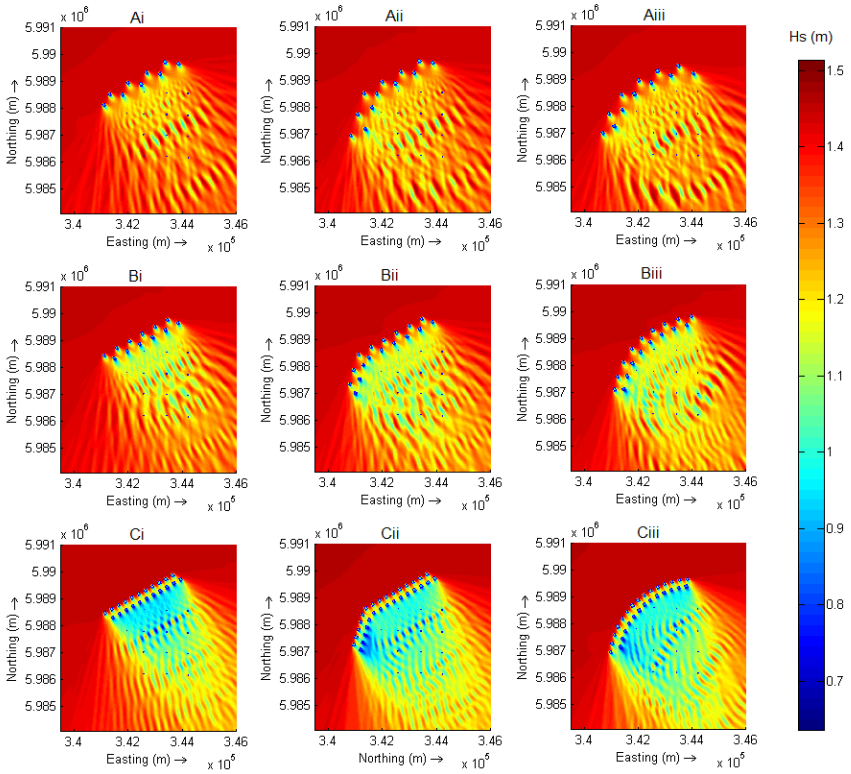

Figure 9. Wave height reduction within the wind farm (*HRF*) for H_s = 1.5 m, T_p = 6.5 m and θ = 330° and configurations A_i to C_{iii}.

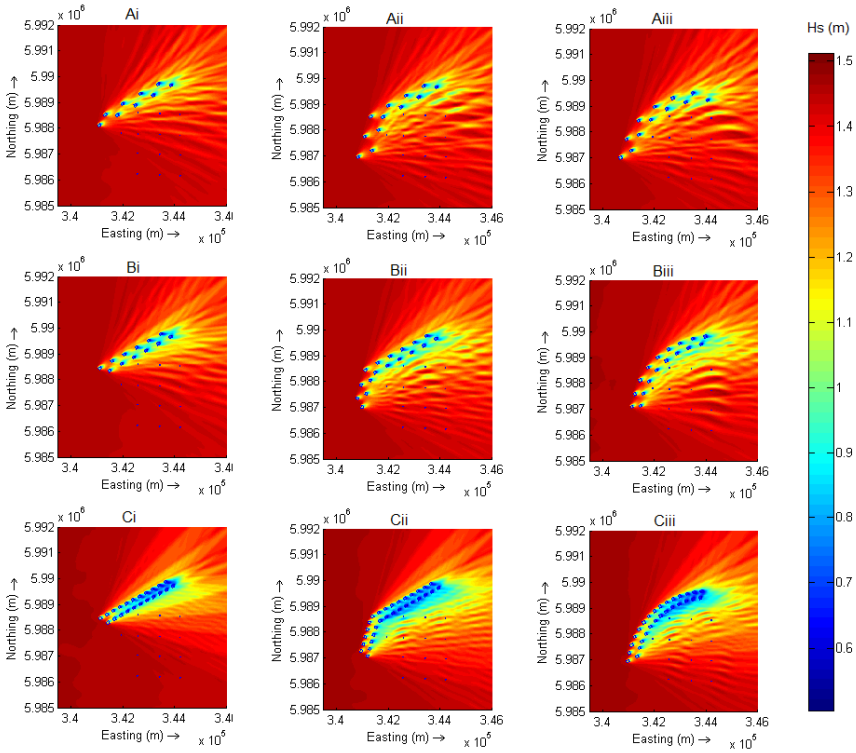

Figure 10. Wave height reduction within the wind farm (*HRF*) for H_s = 1.5 m, T_p = 6.5 m and θ = 250° and configurations A_i to C_{iii}.

Table 8. *HRF* (%) values for CS1 (H_s = 1.5 m, T_p = 6.5 m, θ = 330°) and CS2 (H_s = 1.5 m, T_p = 6.5 m, θ = 250°), and configurations A_i to C_{iii}.

Configuration		N_{WECs}	*HRF* (%)		
			CS1	CS2	Weighted average
A	A_i	9	12	2	9
	A_{ii}	12	13	6	11
	A_{iii}	12	13	4	11
B	B_i	12	14	4	11
	B_{ii}	17	16	9	14
	B_{iii}	17	16	8	14
C	C_i	22	25	5	19
	C_{ii}	30	27	10	22
	C_{iii}	28	26	13	22

In view of the results (Table 9), *HRF* is greater in the new layouts proposed than in the basic cases – C_i, C_{ii} and C_{iii}. This is due to the better interception not only of southwesterly waves but also of northwesterly, due to the superposition of the shadow effects generated by each individual WEC. The maximum reduction was obtained for the configuration C_{iic} (*HRF*= 25%), i.e. the configuration with two rows at an angle of 45° and four additional WECs with respect to C_{ii}. Configuration C_{ic} seems to be a good configuration; however, this result is slightly misleading in that it does not reflect the significant differences in wave exposure within the farm – indeed, this configuration leaves the wind turbines in the northwestern sector of the farm exposed to westerly waves.

To sum up, the lower the spacing between devices, the largest the *HRF* values, and therefore C_x configurations generally lead to larger reductions in wave height. Among them, the configurations C_i, C_{ib} and C_{ic} should be discarded since they leave part of the wind farm unprotected. On the basis of the results, the configurations C_{iic} and C_{iiic}, with *HRF* = 25% and 23% respectively, were selected for further analysis considering the annual data series from January to December 2013. Moreover, *HRF* values considering the annual data series were also obtained for C_{ii} and C_{iii} in order to examine whether adding WECs to the SW of the wind farm is worthwhile. The maximum value of *HRF* achieved was 18%, which corresponds to the configuration C_{iic} (Table 10). However, the arched configuration C_{iiic} yielded a similar wave height

reduction, even though this configuration has 2 fewer WECs than C_{iic}, which is interesting for a future analysis in terms of the total cost. Moreover, it was observed that in both cases – configurations with two rows at an angle and in arch – the addition of 4 WECs to the SW increases the reduction by almost two points.

Table 9. *HRF* (%) values for CS1 (H_s = 1.5 m, T_p = 6.5 m, θ = 330°) and CS2 (H_s = 1.5 m, T_p = 6.5 m, θ = 250°) and configurations C_i to C_{iiic}.

Configuration		N_{WECs}	*HRF* (%)		
			*C*S1	CS2	Weighted average
i	C_i	22	25	5	19
	C_{ib}	27	28	12	23
	C_{ic}	31	29	15	25
ii	C_{ii}	30	27	10	22
	C_{iib}	32	29	13	24
	C_{iic}	34	29	16	25
iii	C_{iii}	28	26	13	22
	C_{iiib}	30	27	15	23
	C_{iiic}	32	27	16	23

Table 10. *HRF* (%) values for the annual serie Data and configurations C_{ii} to C_{iiic}.

Configuration	N_{WECs}	*HRF* (%)
C_{ii}	30	16
C_{iic}	34	17
C_{iii}	28	16
C_{iiic}	32	17

As for the assessment of the augmented weather windows for O&M with co-located WECs, the operational limit for workboats is a significant wave height of 1.5 m. Therefore, the total number of hours when $H_s \leq 1.5$ m was quantified for the study period (Table 11). In the baseline scenario (a standalone wind farm) the total number of hours when $H_s \leq 1.5$ m (T) was 5916 h, which represents 67.5% of the year. With the co-located layouts analysed, this value was significantly increased (Table 11). According to the results of the *HRF* assessment, the best scenario was obtained for configuration C_{iic}, with an increase in the accessibility to the turbines ($\Delta T_{O\&M}$) of approximately 20%. The arched configuration C_{iiic} shows a very

similar increase with 2 WECs fewer (17.8%). In both cases, the accessibility was above 82%, which is the reference value to maintain the wind farm availability above 90% [24].

Table 11. T_{WECs}. accesibility and $\Delta T_{O\&M}$ for configurations C_{ii}, C_{iic}, C_{iii}, C_{iiic}.

Configuration	T_{WECs} (h)	Accesibility(%)	$\Delta T_{O\&M}$ (%)
C_{ii}	7074	80.8	16.4
C_{iic}	7212	82.3	18.0
C_{iii}	6840	78.1	13.5
C_{iiic}	7200	82.2	17.8

The best results were obtained for the configurations with smaller spacing between devices and WECs facing not only the main wave direction (W) but also the secondary wave directions (NW and SW), for these provide a similar wave height reduction in the entire wind farm area. Furthermore, it is worth pointing out that, although the greatest level of accessibility to the wind turbines was obtained for the configuration with WEC rows at an angle, the arched configuration achieved a similar value, despite having two WECs less, which could be an interesting aspect for a future study into cost-effectiveness.

3.3. Comparative Study

The proper functioning of the nearshore wave propagation model was validated with wave buoy data. In all cases, a good correlation was observed between the simulated and measured time series, as shown by the values of R^2 and *RMSE*, always higher than 0.93 and lower than 0.36 m, respectively.

As regards the wave height reduction achieved throughout the farm (*HRF*), it ranged between 13% and 19% (Table 12) and was always larger for the layouts with WECs deployed at an angle than for those in arch, although the difference between the results of both configurations was small (between 1 and 2%).

Comparing the results between wind farms (Table 12), the best values were obtained for Bard 1, where a good interception of the incoming waves was achieved for the two layouts of co-located farms (Figure 11). These results were followed very closely by those obtained for Alpha Ventus and Horns Rev 1, whereas the wave height reduction achieved at Lincs was smaller. This was due to three main factors. First, the wind farm layout – this farm has a slightly elongated shape. Second, the wave direction has a greater

variability than in the other case studies, and the farm remained unprotected against waves from secondary directions (Figure 12). For this reason a larger number of WECs would be required on the east side of the farm to achieve better results; however, this would imply an important increase in the ratio between the number of WECs and wind turbines, raising the final cost of the co-located farm. Third, the wave climate in this park, which was milder than in the other farms and, therefore, less wave energy could be extracted by the co-located WECs.

Table 12. *HRF* (%) values achieved with co-located WECs deployed in angle or in arch based on the annual data series

Wind farm	Layout	N_{WECs}	*HRF* (%)
Alpha Ventus	in angle	34	18
	in arch	32	17
Bard 1	in angle	79	19
	in arch	79	17
Horns Rev 1	in angle	55	17
	in arch	53	15
Lincs	in angle	81	14
	in arch	80	13

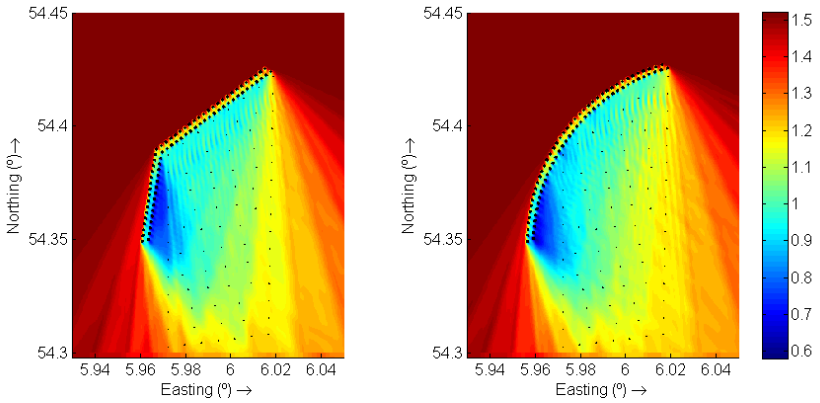

Figure 11. Wave height reduction obtained with co-located WECs at Bard 1 under a sea state with: *Hs* = 1.71 m, *Tp* = 6.09 s and θ = 230º. The colour scale represents the significant wave weight, *Hs* (m).

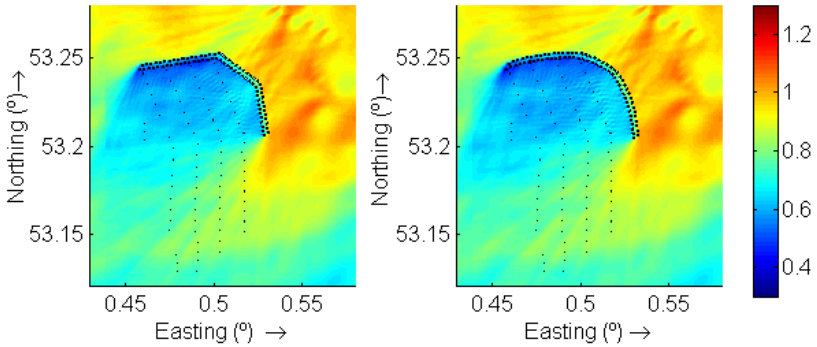

Figure 12. Wave height reduction due to co-located WECs at Lincs under a sea state with: *Hs*= 1.18 m, *Tp*= 6.03 s and θ= 60º. The colour scale represents the significant wave weight, *Hs* (m).

Furthermore, the results of Horns Rev 1 are particularly interesting since they were similar to those of the best scenario, even though the ratio between number of WECs and wind turbines in Horns Rev 1 is much lower than in the other cases – an important consideration for the economic assessment. The explanation lies in the geometry of the wind farms: the layout of Horns Rev 1 is close to a square, whereas Bard 1 or Lincs have a more elongated shape and therefore require more WECs for a similar degree of shelter.

Apart from the average wave height reduction in the farm (*HFR*), it is interesting to analyse the spatial variation in the wave height reduction through its value in different sections (HRA_j), since the best WECs layout should achieve not only high values of *HFR* but also a fairly homogenous reduction throughout the farm. As may be expected, in all case studies the tendency was for the highest reduction to occur immediately behind the WECs, with HRA_j decreasing with increasing distance from the co-located WECs (Figure 13). However, the wave height reduction was significant even as the distance from the WECs increased. As with the wave height reduction for the entire farm, greater values of HRA_j were obtained generally for configurations with WECs deployed at an angle rather than in arch. Lincs presented the highest difference between HRA_j values in the first and second area of turbines (around 23%), and was also the case with the smallest difference between the wave height reduction with co-located WECs in angle or in arch. Therefore, it may be concluded that in the case of wind farms with a milder wave climate, like Lincs, wave heights are restored more quickly behind the WEC barrier, and the choice between

angular or arched layouts for the co-located WECs does not have a significant influence on the enlargement of the weather windows for O&M.

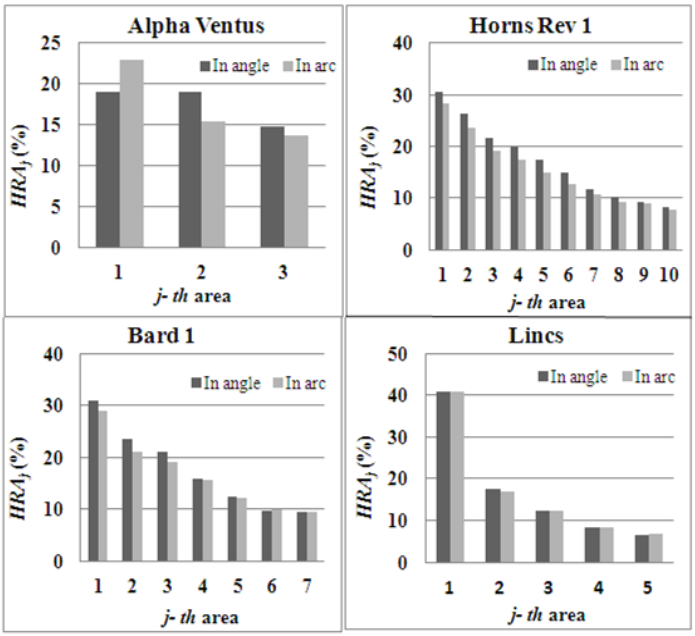

Figure 13. *HRAj* (%) values with co-located WECs deployed in angle or in arch based on the annual data series data.

As regards the accessibility to the wind turbines, it was below 82% for all the wind farms analysed (Table 13), which corresponds to availability values below 90%. Nevertheless, an important increase of the accessibility was achieved by deploying co-located WECs along the periphery of the farm in the four case studies (Table 14). More specifically, the results for Alpha Ventus and Bard 1 were very similar, the accessibility increased ($\Delta T_{O\&M}$) by 17-18%, whereas in Horns Rev 1 this increased by 13-15% and in Lincs by 8%.

Table 13. Accessibility to the wind turbines in the baseline scenario for the annual period analysed.

Wind farm	Accessibility (%)
Alpha Ventus	67.5
Bard 1	57.0
Horns Rev 1	59.9
Lincs	74.1

Table 14. Accessibility and $\Delta T_{O\&M}$ values for the co-located farms considered.

Wind farm	Layout	Accessibility (%)	$\Delta T_{O\&M}$ (%)
Alpha Ventus	in angle	82.3	18.0
	in arch	82.2	17.8
Bard 1	in angle	69.7	18.2
	in arch	69.0	17.5
Horns Rev 1	in angle	70.9	15.6
	in arch	69.5	13.9
Lincs	in angle	81.3	8.9
	in arch	81.1	8.6

4. Conclusions

The aim of this study was to analyse and compare the wave height reduction achieved with different co-located farm layouts and find the configuration that improves the shielding effect of the WECs. To achieve this purpose a number of case studies were considered, using real wave conditions and a third-generation wave model (SWAN). First, an important wave height reduction was achieved in all cases, with significant enlargements of the weather windows for O&M. In fact, in the case of Alpha Ventus and Lincs, values around 82% were obtained for the accessibility, which would ensure an availability of the turbines of 90% or higher. With regard to the influence of the co-located farm layout on the results, the arrays with small spacing between converters achieved the best results of wave height reduction. Moreover, the best results were obtained for co-located wave arrays that face both the prevailing and secondary wave directions, either with WECs deployed in angle or arch. Concerning the influence of the wind farm location, it was found that proximity to land is not a positive factor to implement co-located WECs, since it normally implies lower water depths and a milder sea climate, and consequently there is less available wave energy to be extracted by the WECs. The wind farm layout is another key factor – the largest wave height reduction was achieved for wind farms with square like geometries and smaller spacing between wind turbines, like Horns Rev 1.

In sum, this work: (i) showed that the weather windows regarding wave height are increased as a result of the presence of the wave farm; and (ii) analysed the main aspects to be taken into account in deploying co-located WECs for this purpose.

Acknowledgment

This work was carried out in the framework of the Atlantic Power Cluster project (Atlantic Area Project nr. 2011-1/151, ATLANTICPOWER), funded by the Atlantic Area Operational Transnational Programme as part of the European Regional and Development Fund (ERDF). S. Astariz has been supported by FPU grant 13/03821 of the Spanish Ministry of Education, Culture and Sport. The authors are grateful to: the Bundesamt für Seeschifffahrt und Hydrographie (BSH) of Germany for providing access to the bathymetric and wave data from the FINO 1, 2 and 3 research platforms; to the UK's Centre for Environment, Fisheries and Aquaculture Science (CEFAS) for the wave data from the Dowsign buoy; to the Horns Rev wind farm for the resource data of the site; and to the European Marine Observation and Data Network (EMODnet) for the bathymetric data of the North Sea.

References

[1] S. Astariz and G. Iglesias, "Wave energy vs. Other energy sources: a reassessment of the economics", *International Journal of Green Energy.* In Press (2014).
[2] C. Pérez-Collazo, D. Greaves, G. Iglesias. "A review of combined wave and offshore wind energy", *Renewable and Sustainable Energy Reviews,* vol. 42, pp.141-53, 2015.
[3] C. Pérez-Collazo, M.M. Jakobsen, H. Buckland and J. Fernández-Chozas, "Synergies for a wave-wind energy concept". In EWEA, Frankfurt, Germany, 2013.
[4] S. Astariz, C. Perez-Collazo, J. Abanades and G. Iglesias,"Co-located wind-wave farm synergies (Operation & Maintenance): A case study", *Energy Conversion and Management*, vol. 91, pp. 63-75, 2015.
[5] G.J.W. van Bussel and M.B. Zaaijer, "Reliability, Availability and Maintenance aspects of large-scale offshore wind farms, a concepts stud". In Offshore wind energy special topic conference, Brussels, Belgium, 2001.
[6] Wave Hub. Available at: http://www.wavehub.co.uk/about/location-of-wave-hub/ (13/06/2015).
[7] D.L. Millar, H.C.M. Smith and D.E. Reeve, "Modelling analysis of the sensitivity of shoreline change to a wave farm", *Ocean Engineering*, vol. 34, pp. 884-901, 2007.
[8] J.P. Kenny. "SW Wave Hub- Meteocean design basis". *METOC2009*. p. 111.

[9] TUDelft. "Wind farm optimization, Horns Rev: optimization of layout for wake losses in: T.U". Eindhoven, (Ed.). SET MSc course wind energy2006.
[10] G. Iglesias, H. Fernández, R. Carballo, A. Castro and F. Taveira-Pinto, "The WaveCat© – Development of a new Wave Energy Converter World". Renewable Energy Congress 2011, Linkoping, Sweden, 2011.
[11] H. Fernandez, G. Iglesias, R. Carballo, A. Castro, J.A. Fraguela, F. Taveira-Pinto, et al., "The new wave energy converter WaveCat: Concept and laboratory tests", *Marine Structures*, vol. 29, pp. 58-70, 2012.
[12] G.J. Allan, I. Bryden, P.G. McGregor, T. Stallard, J. Kim Swales, K. Turner, et al., "Concurrent and legacy economic and environmental impacts from establishing a marine energy sector in Scotland", *Energy Policy*, vol. 36 pp. 2734-2753, 2008.
[13] DOTI GmbH (2011). Alpha Ventus Fact Sheet. Available at: http://www.alpha-ventus.de/uploads/media/av_Factsheet_en_May_2011.pdf.
[14] C. Beels, P. Troch, J.P. Kofoed, P. Frigaard, J. Vindahl Kringelum, P. Carsten Kromann, et al., "A methodology for production and cost assessment of a farm of wave energy converters", *Renewable Energy*, vol. 36, pp. 3402-3416, 2012.
[15]http://www.4coffshore.com/windfarms/bard-offshore-1-germany-de23.html (13/06/2015).
[16]http://www.4coffshore.com/windfarms/lincs-united-kingdom-uk13.htm (13/06/2015).
[17] A. Palha, L. Mendes, C.J. Fortes, A. Brito-Melo and A. Sarmento, "The impact of wave energy farms in the shoreline wave climate: Portuguese pilot zone case study using Pelamis energy wave devices", *Renewable Energy*, vol. 35, pp. 62-77, 2010.
[18] H.C.M. Smith, C. Pearce and D.L. Millar, "Further analysis of change in nearshore wave climate due to an offshore wave farm: An enhanced case study for the Wave Hub site", *Renewable Energy*, vol. 40, pp. 51-64, 2012.
[19] J. Abanades, D. Greaves and G. Iglesias, "Wave farm impact on the beach profile: A case study", *Coastal Engineering*, vol. 86, pp. 36-44, 2014.
[20] S. Ponce de Leon, J.H. Bettencourt, N. Kjerstad, "Simulation of Irregular Waves in an Offshore Wind Farm with a Spectral Wave Model", *Continental Shelf Res*, vol. 31, p. 17, 2011.
[21] ETSU, "Potential effects of offshore wind developments on coastal processes", *ETSU W/35/00596/00/REP*. In: P.b.A.a. METOC, (Ed.). http://www.offshorewindenergy.org/reports/report_002.pdf, 2002.
[22] S. Astariz, C. Perez-Collazo, J. Abanades and G. Iglesias, "Towards the optimal design of a co-located wind-wave farm", *Energy*, vol. 84, pp. 15-24, 2015.
[23] T. Hayashi, Hattori, M., Kano, T., Shirai and M, "Hydraulic Research on the Closely Spaced Pile Breakwater", *Coastal Engineering*, vol. 50, p.12, 1966.
[24] G.J.W. van Bussel, W.A.A.M. Bierbooms, "The DOWEC Offshore Reference Windfarm: analysis of transportation for operation and maintenance", *Wind engineering*, vol. 27, p. 11, 2013.